

Localized Corrosion of Mild Steel under Silica Deposits in Inhibited Aqueous CO₂ solutions

Jin Huang, Bruce Brown and Srdjan Nesic

Institute for Corrosion and Multiphase Technology
342 west State Street
Athens, OH, 45701
USA

ABSTRACT

Corrosion experiments were conducted on API 5L X65 mild steel specimens covered by a silica deposit in inhibited 1 wt% NaCl aqueous solutions saturated by CO₂ at pH 5.0 and 25°C. It was observed that a generic imidazoline based inhibitor was not able to reduce the general corrosion rate of the steel underneath the silica sand particles and local acceleration of corrosion (pitting) was found in those areas. A pitting penetration rate was calculated using Infinite Focus Microscopy (IFM) measurements. After examining many possible mechanisms, it was concluded that the imidazoline inhibitor was not depleted globally by adsorption on the sand surface and that it did diffuse through the sand deposit to reach the steel surface. However, locally - immediately underneath each sand grain, the inhibitor preferentially adsorbed on the silica surface, leaving the steel beneath it unprotected. This led to formation of galvanic cells and to accelerated localized corrosion at those locations.

Key words: CO₂ corrosion, silica deposit, mild steel, pit, localized corrosion, mechanisms

INTRODUCTION

In upstream oil and gas pipelines, when the flow rate is low, solids (including silica sand) may deposit on the bottom of the line and form a layer. Observations of accelerated corrosion in these conditions have led to the need to better understand the causes and corrosion mechanisms involved in this so called *under-deposit attack*. It is known that a layer of solids creates unique conditions underneath it, where the water chemistry is different from the adjacent areas of the steel exposed to the bulk solution. It also appears that the deposit limits the access of corrosion inhibitors to the metal surface, although it is not clear how and why this happens.

A variety of speculations have been published on how inhibitor efficiency is affected by solid deposits.¹⁻⁹ Pedersen *et al.*² suggested that the inhibitor lost efficiency due to adsorption onto the large surface area of a sand deposit. Turnbull *et al.*⁷ believed that the poor efficiency of the inhibitor they used was

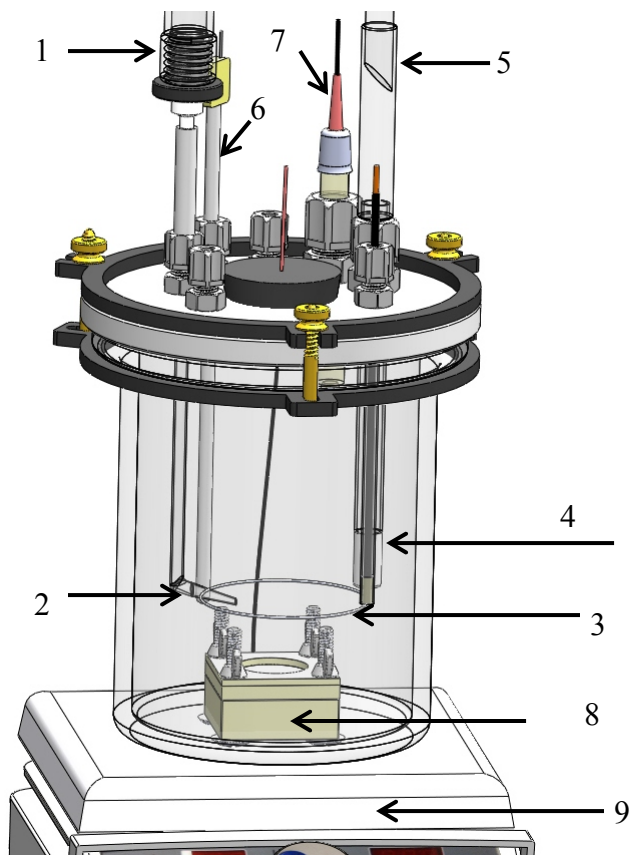
due to slow diffusion of the inhibitor through the deposit layers. Crossland *et al.*⁸ found accelerated corrosion underneath the deposit; however, no mechanisms were proposed.

In a previous study, the present authors (Huang *et al.*¹) tested the effect of silica sand deposits on CO₂ corrosion mechanisms of mild steel in an inhibitor-free system and found that under those conditions the porous sand deposit retards corrosion of the steel underneath. In the present study, the work has been extended to cover the effect of inhibitors.

EXPERIMENTAL METHOD

Test setup: experiments were conducted at atmospheric pressure in a three-electrode glass cell setup, as shown in Figure 1. A concentric ring made from platinum wire was used as the counter electrode (CE). A KCl saturated silver-silver chloride (Ag/AgCl) electrode was chosen as the reference electrode (RE) and was connected to the test solution externally *via* a Luggin capillary. The working electrode (WE) specimen was a cylindrical carbon steel disc, shown in Figure 2. A temperature probe was connected to a heater to control the test solution temperature. A glass pH probe was also immersed in the solution to monitor the bulk pH during the test. CO₂ gas was purged into the test solution before and during each test to maintain a de-oxygenated and a CO₂ saturated environment. The test solution was: two liters of DI water with 1 wt% sodium chloride (NaCl). The WE was mounted onto a holder which was connected with CE and RE to a potentiostat for electrochemical measurements during the test. The general corrosion process was monitored using electrochemical techniques including linear polarization resistance (LPR) and electrochemical impedance spectroscopy (EIS). After the experiments, the specimen surface morphology was analyzed by using a scanning electron microscope (SEM) and the localized corrosion was investigated using infinite focus microscopy (IFM).

Steel Specimen: API 5L X65 pipeline steel was used to make WE specimens for all corrosion tests. The exposed area of the specimen was 8 cm². The chemical composition of this pipeline steel is listed in TABLE 1. The specimens were machined from the parent material into cylindrical discs of 3 mm thick and 3.1 cm diameter, as shown in Figure 2. A plastic specimen holder was designed to limit the wetted area to only the upper face of the specimen and provide an easy way to place a bed of sand on top. The holder consists of three parts: the base, the specimen holder and the deposit holder (see Figure 2). Note the spring-pin connectors for electrical connection in the base and an O-ring around the perimeter of the specimen holder used to seal against leaks. When mounted in the specimen holder, the specimen's upper surface is flush with the holder. A plastic deposit holder (from 2 to 10 mm high), is then placed on top of the specimen holder and locked into place. Once installed, the deposit is poured to fill the available volume of the deposit holder.



1. Reference electrode.
2. Luggin capillary.
3. Platinum Counter electrode.
4. CO₂ gas inlet.
5. Condenser.
6. Thermal probe.
7. pH probe.
8. Specimen holder
9. Heater

Figure 1: Three-electrode glass cell setup.

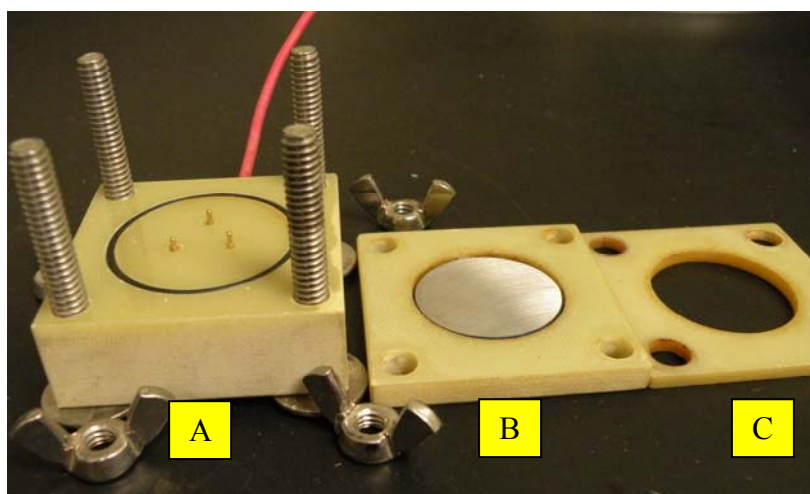


Figure 2. API 5L X65 carbon steel specimen holder: (A) base, with three gold contacts to connect the steel specimen and wire for electrochemical measurement; (B) steel sample holder, where steel specimen is installed; (C) sand holder, fill up to 2 mm sand deposit.

TABLE 1 Chemical composition of API 5L X65 mild steel (mass % balance is Fe)

Al	As	B	C	Ca	Co	Cr	Mn	Mo	Ni	Nb
0.032	0.008	0.001	0.13	0.002	0.007	0.14	1.16	0.16	0.36	0.017
P	Pb	S	Sb	Si	Sn	Ta	Ti	V	Zr	Cu
0.009	<0.001	0.009	0.009	0.26	0.007	<0.001	<0.001	0.047	<0.001	0.131

Solid Deposit: silica sand was used as the solid deposit and two different particle sizes were chosen: 750 μm and 250 μm . SEM images of these particles are shown in Figure 3. Unless specified otherwise, deposits were cleaned with DI water and were stored in test solution saturated by CO_2 prior to testing. A pipette was used to transfer the deposit material onto the corroding specimen for each test. The transfer process took less than 10 seconds in order to minimize oxygen contamination of the transferred sand. No indication of iron oxide was ever found in these tests.

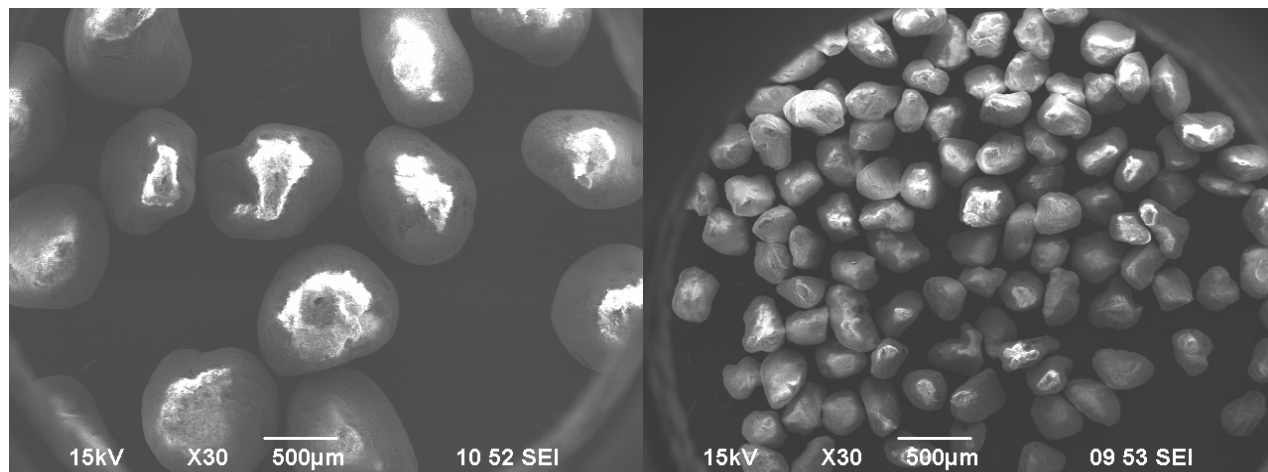


Figure 3. SEM images of silica particles with different size: 750 μm (left), 250 μm (right).

Corrosion Inhibitor: a corrosion inhibitor, designated “K1”, was used in this study. K1 is an imidazoline-based generic inhibitor with 24% (wt. %) active TOFA/DETA. The critical micelle concentration (CMC) for this inhibitor was experimentally determined by using a tensiometer.¹⁰ The key information about the K1 is summarized in Table 2. It is known from previous experimentation that K1 is able to effectively retard bare steel corrosion by physically adsorbing onto the steel surface.¹¹

Table 2: Inhibitor information.

Inhibitor	Components	CMC (in 1 wt% NaCl)	Concentration used here
K1	24% TOFA/DETA + 10% glacial acetic acid + 53% DI water	36 ppm	70 ppm

Test Procedure: the test solution was heated to the desired temperature and at the same time deoxygenated by continuously purging with CO_2 gas for at least 1 hour. Once the test solution was saturated with CO_2 , the pH of the solution was adjusted to the designated value by adding either a de-oxygenated sodium bicarbonate (NaHCO_3) or a de-oxygenated hydrochloric acid (HCl) solution. The pH was monitored and recorded regularly. After the test solution was prepared, the API 5L X65 test specimen was polished with 200, 400 and 600 grit sand paper sequentially under a continuous rinse by isopropyl alcohol and air dried. The specimen was then mounted onto the specimen holder and immersed into the prepared test solution, and the test was started.

Initially, the API 5L X65 specimen was corroded for 24 hours without a deposit, while the open circuit potential and the general corrosion rate (as measured by LPR) were monitored. Electrochemical impedance spectroscopy (EIS) measurements were also conducted to determine the solution resistance in order to compensate the polarization resistance for the IR drop in the solution (this was done manually during post-processing of the data). This electrochemical response of the bare steel was taken as a reference behavior for later evaluation of the deposit effects. In each under-deposit

corrosion test, the specimen was first corroded without a deposit for an hour (pre-corrosion), while the open circuit potential, corrosion rate (LPR) and solution resistance (EIS) was recorded. The test proceeded to the under-deposit stage only when the initial bare steel corrosion process was in the expected range. After the deposit was added, the open circuit potential, corrosion rate (LPR) and solution resistance (EIS) was monitored once every two hours until the end of the test. At the end, the test, the specimen was taken out of the solution, rinsed (dehydrated) with isopropyl alcohol, dried with cool air, and stored in a desiccator for surface analysis (SEM and EDX). Clarke solution¹² was used to remove the corrosion product layer from the specimen surface and IFM was used to measure the localized pit penetration rate.

Table 3: Experimental conditions.

Parameter	Conditions
Test material	API 5L X65 mild steel
Test solution	DI water + 1wt% NaCl
Temperature	25°C & 80°C
CO ₂ partial pressure	0.96 bar & 0.54 bar, respectively with temperature
Solution pH	5
Deposit	Silica sand
Sweep rate	0.125 mV/s
Polarization resistance	From -5 mV to 5 mV vs. E_{oc}
AC impedance	± 5 mV vs. E_{oc} from 5 kHz to 1 mHz

During the LPR measurements, the WE was polarized ± 5 mV from the open circuit potential (E_{oc}) at a scan rate of 0.125 mV/s to obtain the polarization resistance (R_p) which was then used to calculate the general corrosion rate of the steel. For the EIS measurement, a sinusoidal potential signal ± 5 mV peak-to-peak around E_{oc} was applied to the working electrode with scanning frequencies from 5 kHz to 1 mHz. Experimental conditions are summarized in Table 3.

RESULTS AND DISCUSSION

K1 performance: imidazoline has been known as an inhibitor for CO₂ corrosion of carbon steel.^{11, 13} To compare the effect of sand deposit on K1's performance, the inhibitor efficiency of K1 on bare steel was firstly tested.

Figure 4 shows the variation of general corrosion rate with time obtained from LPR measurements. It can be seen that the corrosion rate dropped dramatically after the addition of 2 CMC K1. The presence of K1 induced a 50 mV increase in corrosion potential while the corrosion rate decreased to about 0.15 mm/y after 25 hours achieving 90% inhibitor efficiency. The results of inhibition performance on bare steel were consistent with previous work¹⁰, which shows the appropriateness of the inhibitor K1 used for the current study.

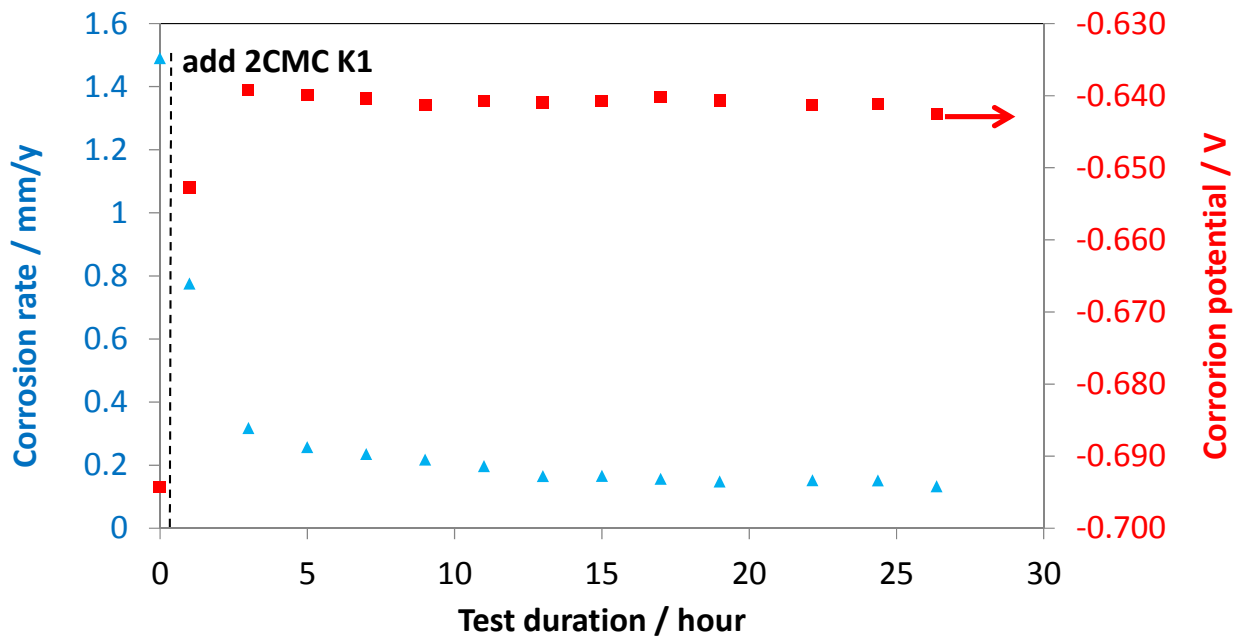


Figure 4: Corrosion rate and corrosion potential of mild steel measured with LPR at 25°C, pH 5 with 70 ppm (2 CMC) K1.

The performance of K1 on mild steel in the presence of 2 mm silica sand deposit was then studied and compared to the same test done with bare steel. The variation of corrosion rate under conditions with sand deposit is shown in Figure 5. It can be seen that the sand deposit had a significant effect on K1's performance. In the presence of this sand deposit, the addition of K1 didn't reduce the general corrosion rate of mild steel as it did on the bare steel surface (final corrosion rate: 0.45 mm/y vs. 0.15 mm/y).

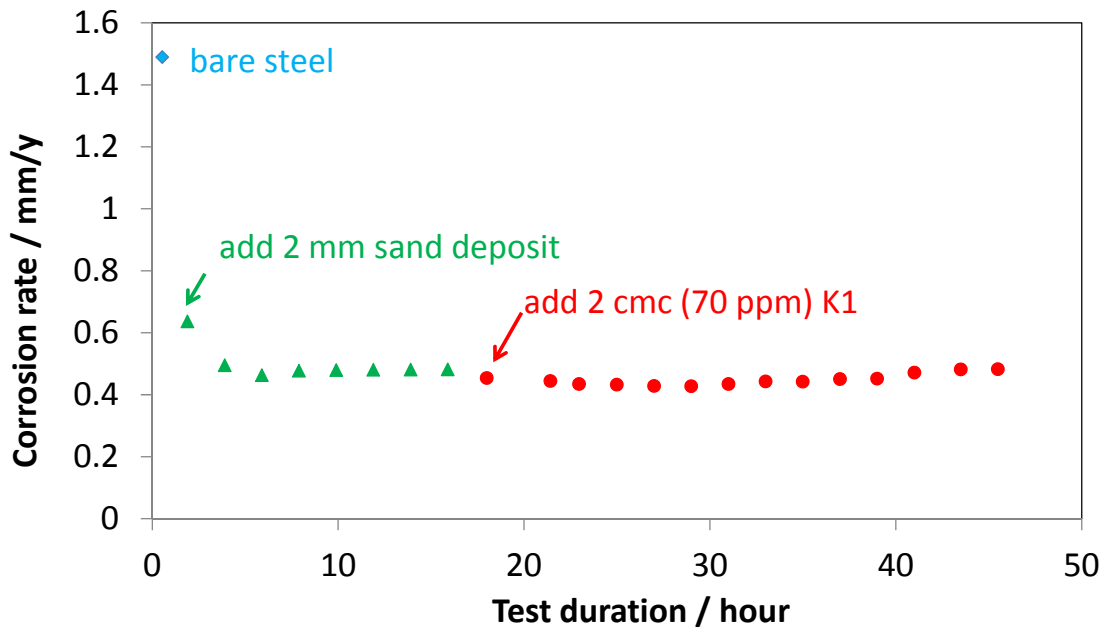


Figure 5: Corrosion rate of mild steel measured with LPR at 25°C, pH 5.

Mechanism: the observation that the imidazoline based inhibitor K1 had no effect on the general corrosion rate of mild steel in the presence of a sand deposit is in general agreement with other reported work.^{6, 8} Place⁶ and Crossland⁸ also found that treating the bulk electrolyte with inhibitors had no effect on the corrosion rate underneath a deposit. However, it has been reported elsewhere that, even with a solid deposit present, some inhibitors still worked very well^{4, 7}

For the cases when the inhibitors do not perform in the presence of sand deposits, it is commonly believed that the large surface area of the deposit depletes the inhibitor, therefore making it unavailable to adsorb onto the steel surface underneath the deposit.² This hypothesis was tested first:

Hypothesis A: Adsorption of inhibitor on the sand surface caused general depletion of the inhibitor and failure to inhibit.

To test this hypothesis, the following experiments were conducted:

The sand deposit was removed from the steel surface at the end of the test. In this case, it was expected that, if Hypothesis A is true, the inhibitor should still not perform, as it was already consumed by adsorption onto the sand. Figure 6 shows the variation of corrosion rate of mild steel with time. After one hour of bare steel pre-corrosion, only one layer of sand was added and then 2 CMC of inhibitor K1 was added after another 24 hours. At the end of the experiment the sand was removed. The LPR corrosion rate data, suggest that once the sand was gone from the steel surface, good inhibition was obtained as would be obtained on a bare steel surface. This experiment has proven that the K1 inhibitor was not depleted by adsorption onto the sand, and that this mechanism cannot be used to explain K1's failure to reduce the corrosion rate of steel covered by sand.

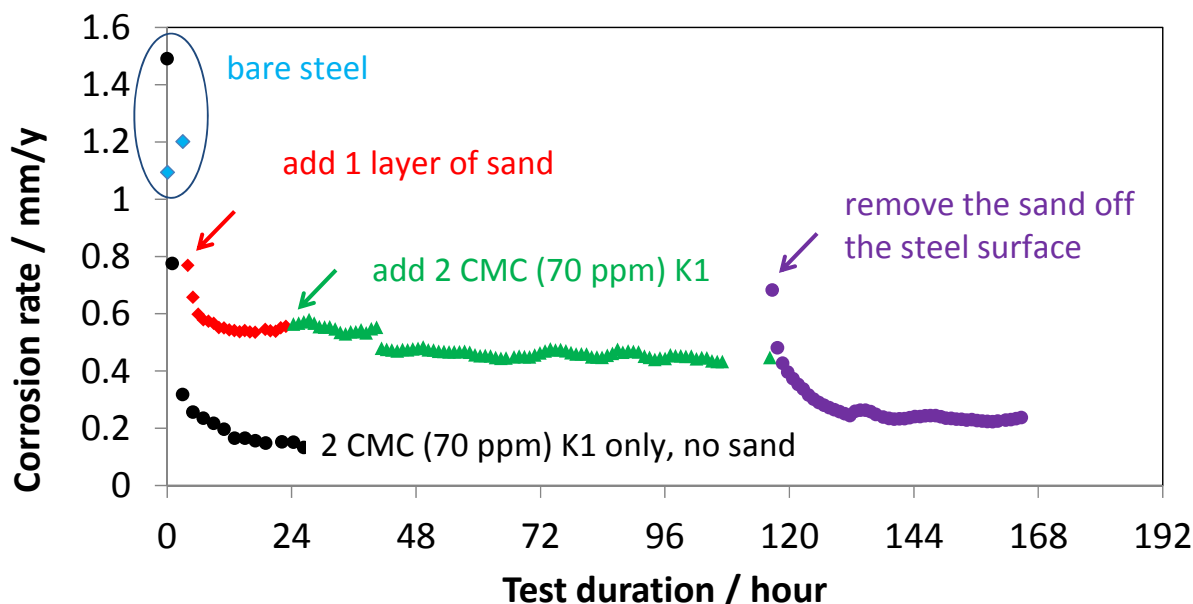


Figure 6: Variation of general LPR corrosion rate with time at test conditions: 1 wt% NaCl solution, bulk pH 5.0, 25°C.

The sand deposit surface charge was altered. The silica sand surface is normally more negatively charged,¹⁴ thereby attracting the more positively charged parts of the inhibitor molecule to adsorb onto it. It was thought that if the surface charge is altered the amount of inhibitor adsorbed onto the silica sand would change. The silica sand was therefore washed by different solutions in order to change the surface charge and change the adsorption of the inhibitor molecules. Dichlorodimethylsilane is believed to have the ability to change the silica surface charge from negative to neutral.¹⁵

Figure 7 shows the variation of corrosion rate of mild steel with time under various sand deposits which were pretreated differently. All deposits were added after one hour of bare steel corrosion. The short vertical lines shown indicate the moment when inhibitor K1 was added. The LPR corrosion rate data indicate no effect on corrosion rate by inhibitor K1 in the presence of the sand deposit, no matter how the deposit surface was pre-treated. The differences between the pre-treated sand deposits are summarized in Figure 8.

The results from these two experimental series clearly disproved the Hypothesis A that: “adsorption of inhibitor on the sand surface causes general depletion of the inhibitor and failure to inhibit.” Other possibilities had to be explored.

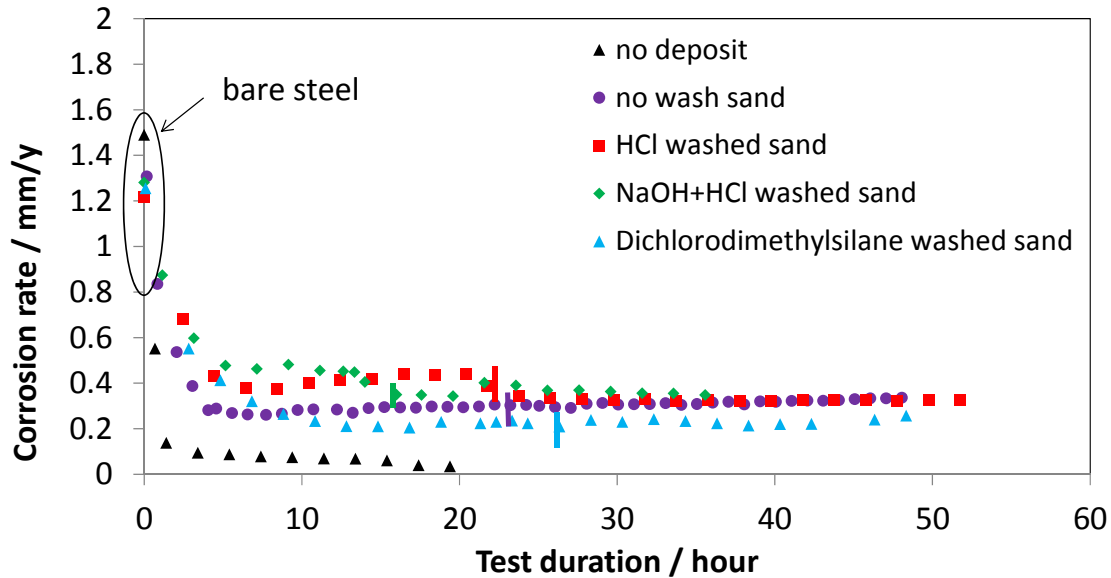


Figure 7: Variation of general LPR corrosion rate with time for different pre-treated silica sand deposits. Test condition: 1 wt% NaCl solution, pH 5 and 25°C.

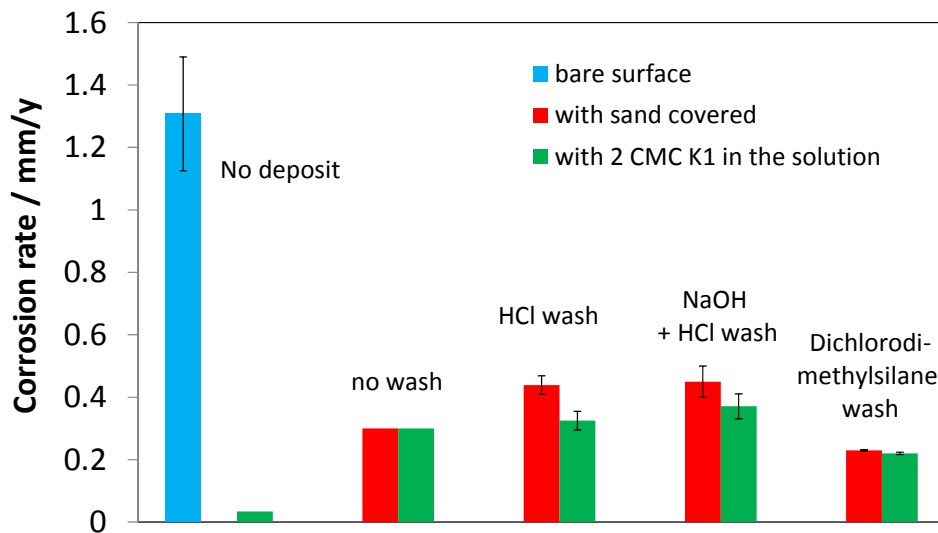


Figure 8: Comparison of general LPR corrosion rate under different pre-treated sand deposits. Test condition: 1 wt% NaCl solution, pH 5 and 25°C.

Hypothesis B: slow diffusion of inhibitor through the sand deposit is the limiting factor that causes inhibitor failure.

The other popular belief is that the poor efficiency of the inhibitor in the presence of sand deposits is due to slow diffusion of the inhibitor through a porous deposit layer.⁷

One can simply express diffusion through a porous layer by using on Fick's law:

$$N = -D_{eff} \frac{\Delta C}{\Delta x} \quad (1)$$

Therefore, if Hypothesis B is correct, increasing the rate of diffusion through the sand deposit (N) should result in better inhibition. This can be easily accomplished by increasing the effective diffusivity (D_{eff}), by increasing the inhibitor concentration gradient across the sand deposit (ΔC), or by decreasing the depth of the porous sand deposit (Δx). Three series of tests were conducted at conditions designed to accelerate the inhibitor diffusion process.

The diffusion coefficient D_{eff} was increased. This was achieved by:

- (a) using larger sand particles for the deposit, having larger porosity and tortuosity (i.e. larger open spaces between sand particles for inhibitor to diffuse).
- (b) conducting experiments at a higher temperature, (80°C).

Larger sand particles: Figure 9 shows the variation of corrosion rate with time for two layers made up of very different particle sizes (250 μm and 750 μm , as shown in Figure 3). No difference was observed in terms of general corrosion rate obtained by LPR - in both cases the sand deposit layer prevented inhibition by K1 in a similar way.

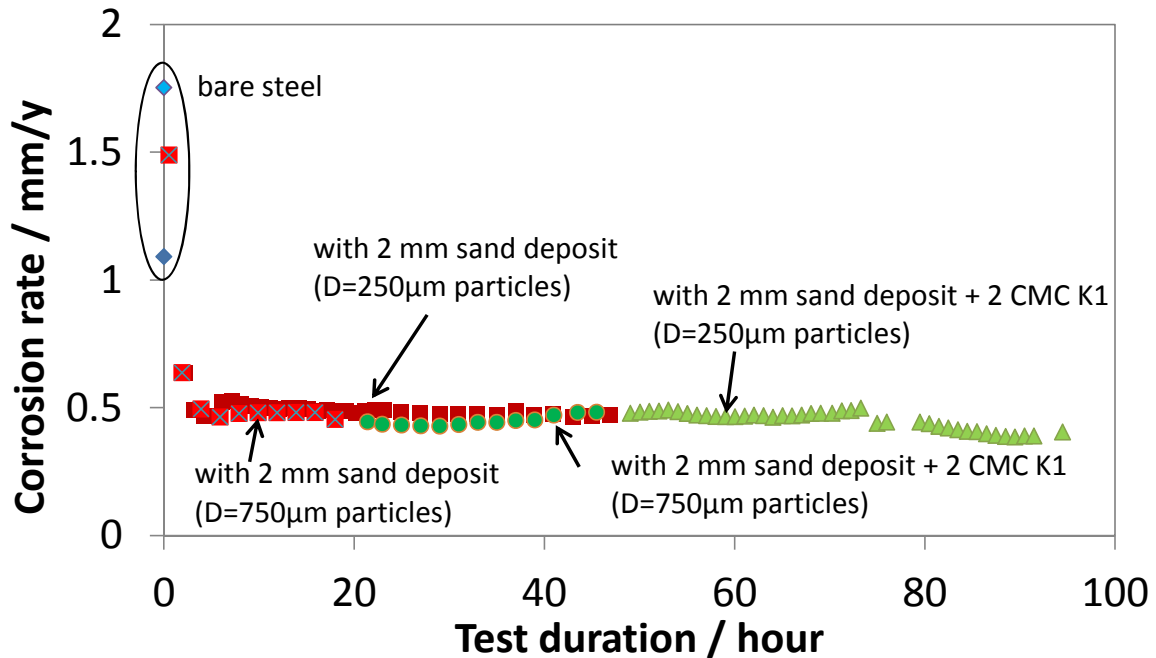


Figure 9: Variation of general corrosion rate with time measured by LPR for two different sizes of sand particles at test conditions: 1 wt% NaCl solution, bulk pH 5.0, 25°C.

Higher temperature: The diffusion coefficient in liquids can be estimated by using the Stokes-Einstein equation:¹¹

$$D = \frac{kT}{3\pi\mu d} \quad (2)$$

where k is the Boltzmann constant, T is the absolute temperature, d is the diameter of the inhibitor molecule, and μ is the viscosity of the liquid; indicating that an increase in temperature will increase the diffusion coefficient. A new series of tests were performed at 80°C. The variation of corrosion rate with time measured from LPR is shown in Figure 10. Little effect of inhibitor was observed in the presence of the sand deposit even at this high temperature.

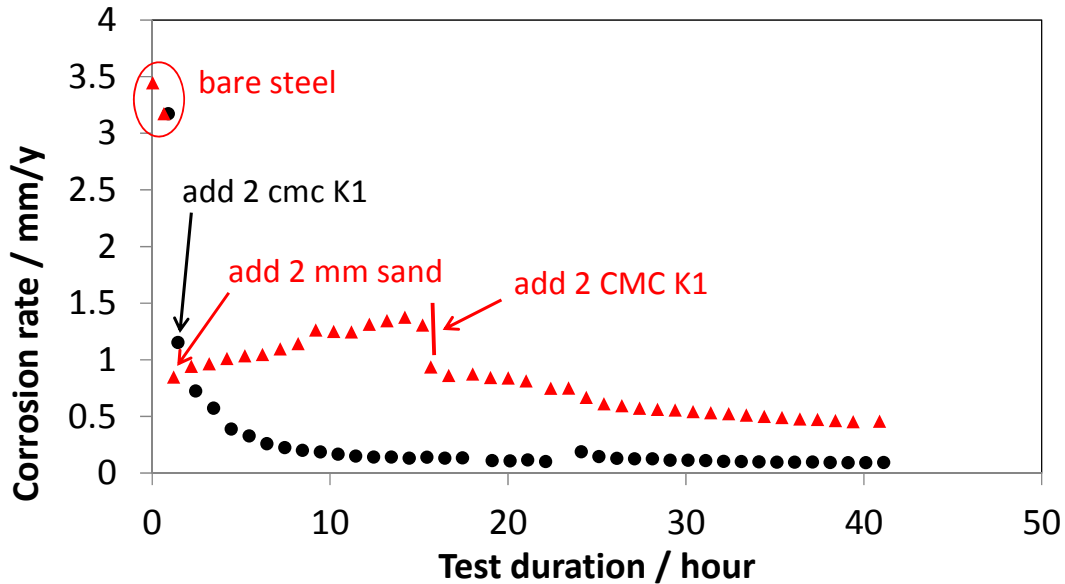


Figure 10: Variation of general corrosion rate with time measured by LPR with at test conditions: 1 wt% NaCl solution, bulk pH 5.0, 80°C.

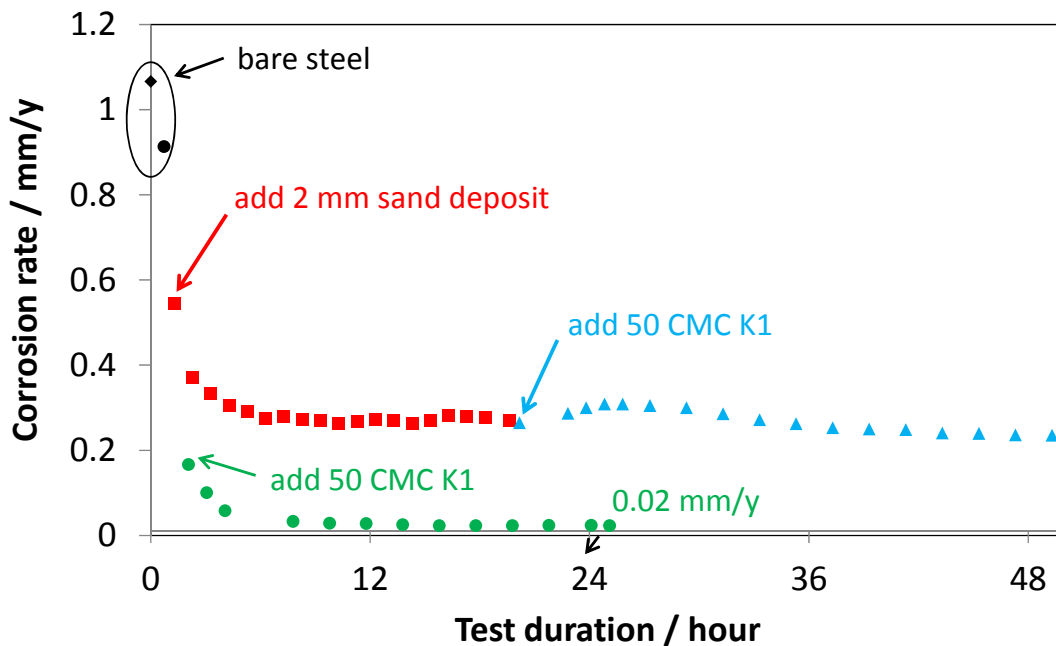


Figure 11: General Corrosion rate of mild steel measured with LPR at 25°C, pH 5.

The driving force ΔC for diffusion was increased by increasing the bulk concentration of inhibitor. In previous tests, 2 CMC K1 was used. Now 50 CMC K1 was used in order to have an extreme driving force for inhibitor diffusion assuming that this was the limiting factor. Figure 11 shows the variation of corrosion rate with time in the presence of 2 mm sand deposits and with 50 CMC K1 added. The behavior was similar as before - poor inhibition was achieved.

The diffusion path Δx for diffusion was decreased. This was achieved by using less sand. 2 mm sand deposit consists of sand particles with average size of 250 μm is roughly 8 layers of sand. The 70% coverage was achieved with the sand particles scattered on the steel surface with approximately 30% of the steel surface area directly exposed to the test solution.

The corrosion rates for these different cases are shown in Figure 12. It shows that one layer of sand was as detrimental for the performance of the inhibitor as were the 10 layers of sand. Furthermore it appears that as long as there was any sand on the steel surface, the inhibitor efficiency was affected.

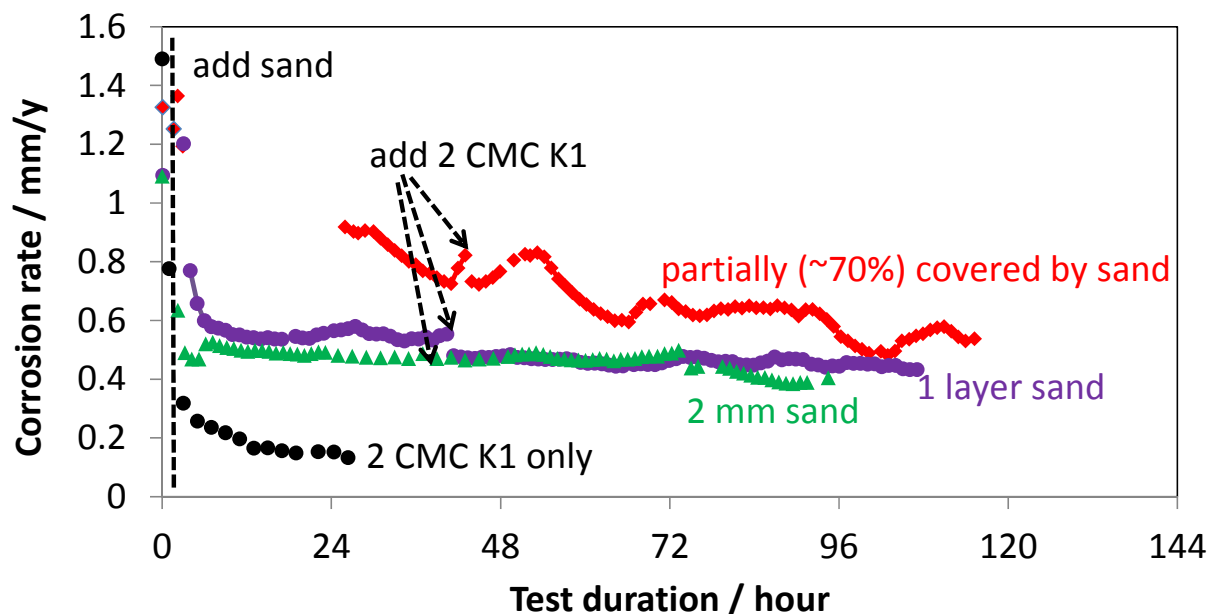


Figure 12: Variation of the general corrosion rate of mild steel with time with different amount of sand deposit, as measured by LPR at 25°C, pH 5.

From the different series of tests described above, *Hypothesis B* could also be rejected and it was confirmed that diffusion of inhibitor through a sand deposit towards the steel surface is not the limiting factor.

It came as surprise though, that even partial (70%) coverage with a single layer of sand lead to poor inhibition. This was followed up on by surface analysis and pits were found on the steel surface. Actually pits were present in several cases described above. Therefore, the emphasis shifted to localized corrosion.

Localized corrosion

CASE 1: One layer of sand, full surface coverage, 2 CMC K1 added after sand.

This case is represented by the LPR data in Figure 6. A single layer of sand was added after one hour of bare steel corrosion, followed by 2 CMC K1 added 24 hours after the sand deposit, and then the deposit was removed after approximately 90 hours, followed by another 24 hours without the sand layer. The steel surface covered by 1 layer of sand is imaged in Figure 13(a). The SEM image of steel

surface after corrosion is shown in Figure 13(b). Pits can be found at many locations across the specimen surface. From IFM analysis (Figure 14), the average pit depth was 35 μm , which is equal to a corrosion rate of 2.0 mm/y. This pit penetration rate is 10 times greater than the general corrosion rate calculated from LPR (Figure 6).

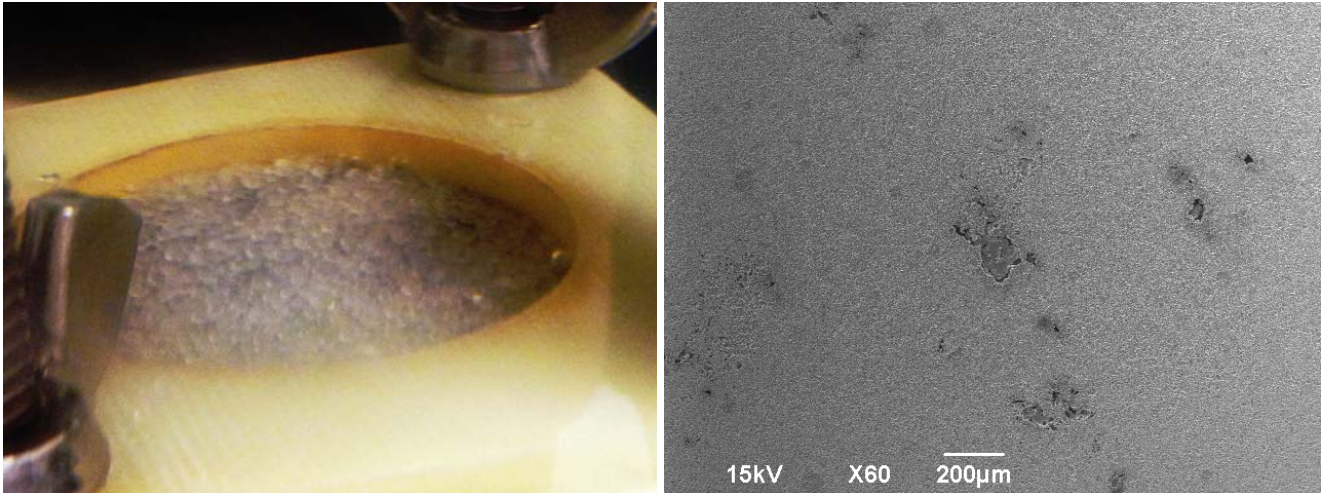


Figure 13: (a) 1 layer of sand deposit on steel surface (b) SEM of steel surface after corrosion product been removed by Clarke solution.

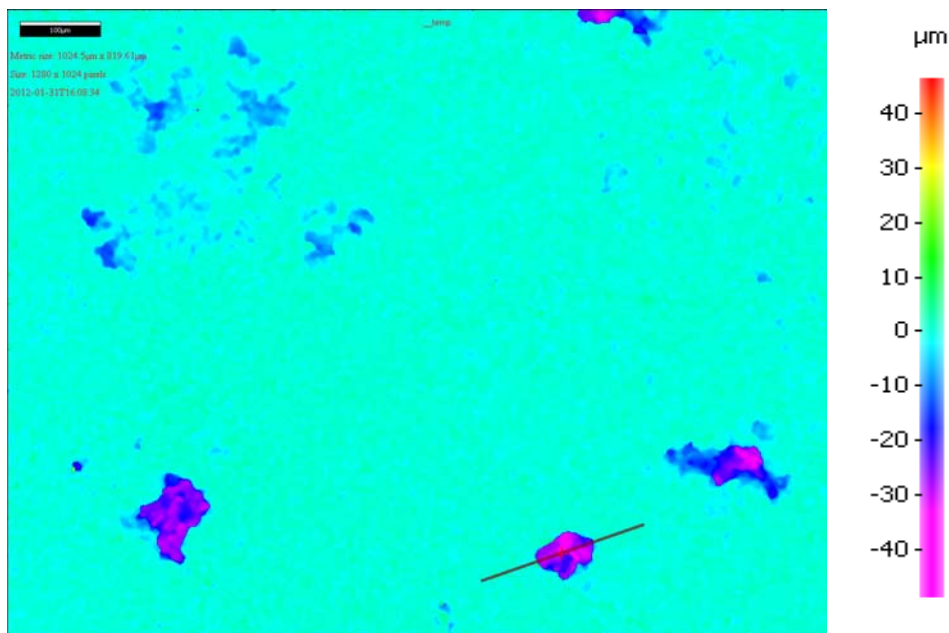


Figure 14: IFM analysis of pits on steel surface.

CASE 2: One layer of sand, scatter sand particles (about 70% coverage), 2 CMC K1 added after sand. In this case, less sand was added on the steel surface so that only about 70% of the steel surface was covered by sand particles. The LPR data for this experiment is shown in Figure 15. After one hour pre-corrosion, the sand was added on the surface, after 24 hours 2 CMC K1 was added, and the corrosion rate observed for 72 more hours before removal of the sand and observation for another 48 hours. Specimen surface analysis shows that pits were found underneath the sand particles. Figure 16(a) shows the morphology of the steel surface after sand particles were rinsed off. Figure 16(b) is the SEM image of steel surface before corrosion product removal by Clarke solution. The general corrosion rate measured by LPR is presented in Figure 15 as well. The general corrosion rate decreased from 0.4

©2013 by NACE International.

Requests for permission to publish this manuscript in any form, in part or in whole, must be in writing to NACE International, Publications Division, 1440 South Creek Drive, Houston, Texas 77084.

The material presented and the views expressed in this paper are solely those of the author(s) and are not necessarily endorsed by the Association.

mm/y to 0.35 mm/y with 2 CMC K1's inhibition. The pit penetration rate was calculated from IFM analysis (Figure 17) to be 2.0 mm/y as most of pits have a depth of 40 μm . This is about 6 times of LPR general corrosion rate 0.3 mm/y during the last 48 hours of the test time.

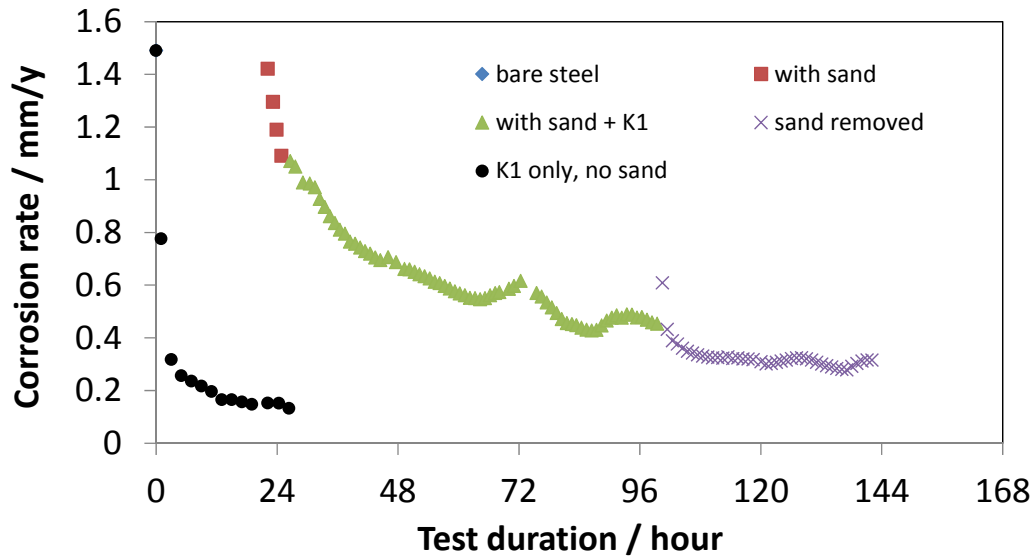


Figure 15: Variation of general corrosion rate with time measured by LPR at test conditions: 1 wt% NaCl solution, bulk pH 5.0, 25°C.

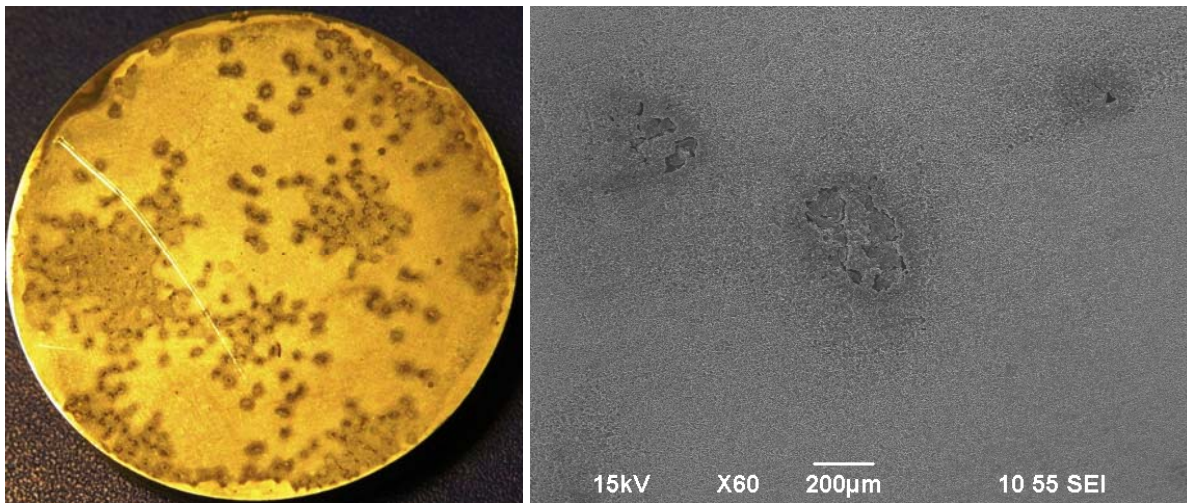


Figure 16: a) Steel surface morphology after rinsing with isopropanol. b) SEM of steel surface after corrosion product removal using Clarke solution.

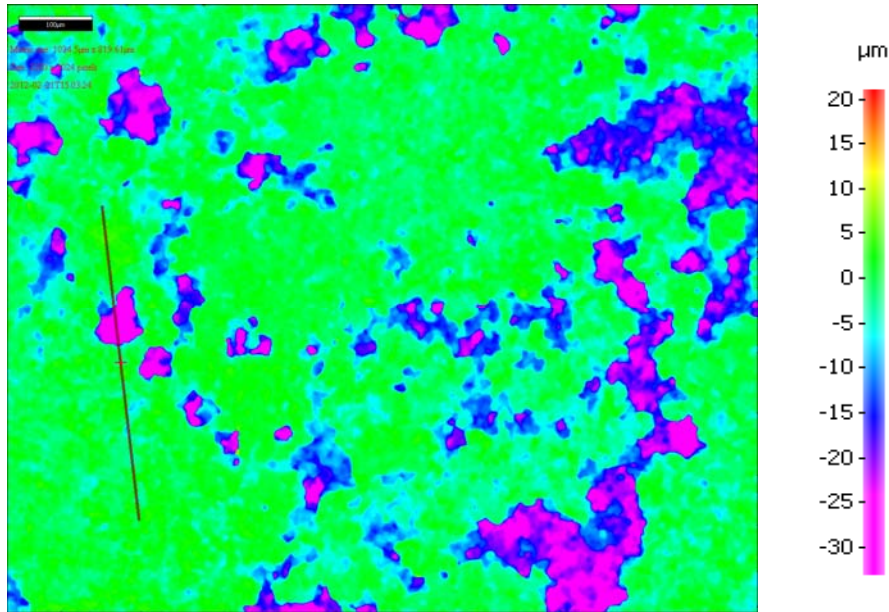


Figure 17: Steel surface morphology analyzed by IFM showing a lot of pits on the steel surface.

CASE 3: Multiple layers of silica sand (2 mm), full coverage, 2 CMC K1 added before sand.

In this case, the steel surface was fully covered with 2 mm deposit. But the 2 CMC K1 was added before the sand deposit was present. The sand deposit was lifted off the steel surface and the corrosion process proceeded for another 20 hours before test ended. Surprisingly, lots of pits were found by SEM analysis (Figure 18). The maximum pit depth was measured to be 45 µm from IFM (Figure 19). The whole steel surface was also scanned by IFM and 90% of pits were found to be having a depth of 40 µm equal to a corrosion rate of 2.2 mm/y. This pit penetration rate is about 30 times greater than the LPR measured general corrosion rate (Figure 20).

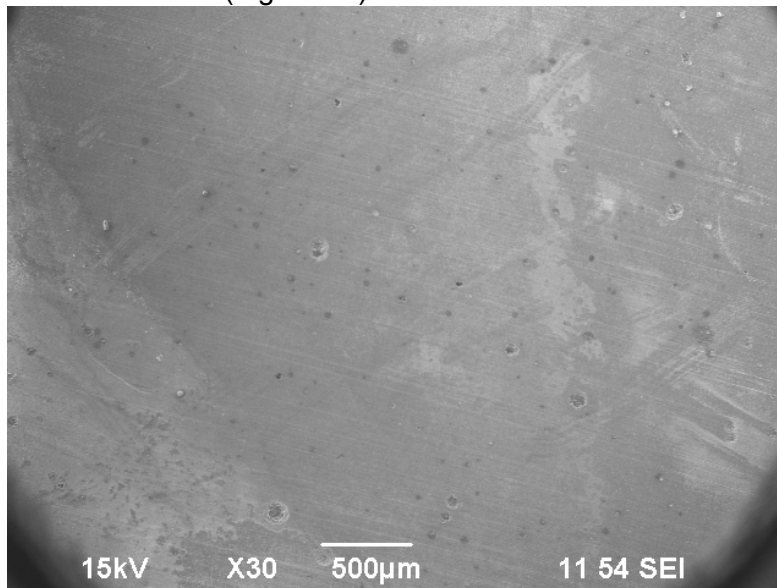


Figure 18: SEM image of test specimen showing pits developed on the steel surface.

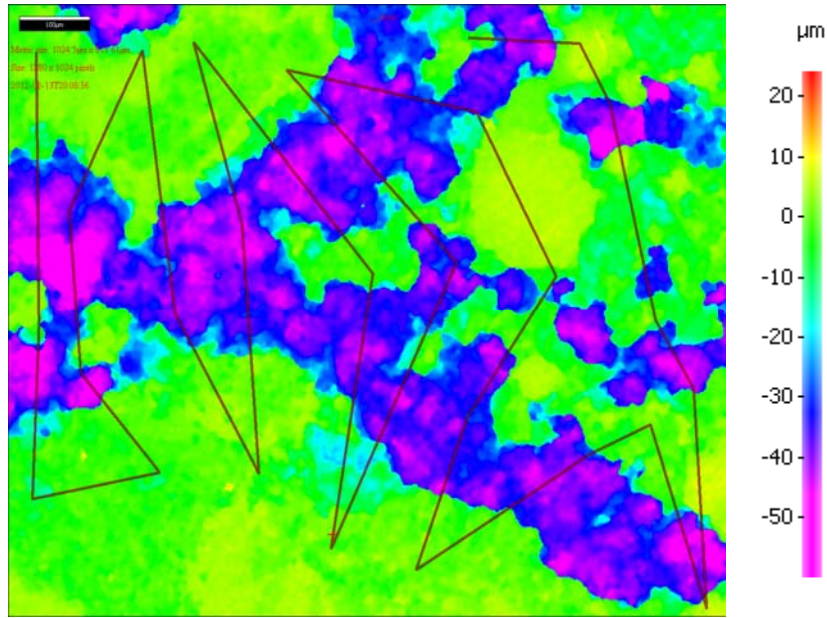


Figure 19: Variation of general corrosion rate with time measured by LPR at test conditions: 1 wt% NaCl solution, bulk pH 5.0, 25°C.

In summary, the cases where pits were found are listed in Table 4. The pit penetration rate and corresponding general corrosion rate measured from LPR are compared. It can be seen that it did not matter whether the steel surface was inhibited before the addition of the deposit, and it did not matter if the steel surface was fully covered by sand particles or not, pitting corrosion was found. And those pits were all found underneath individual sand particles.

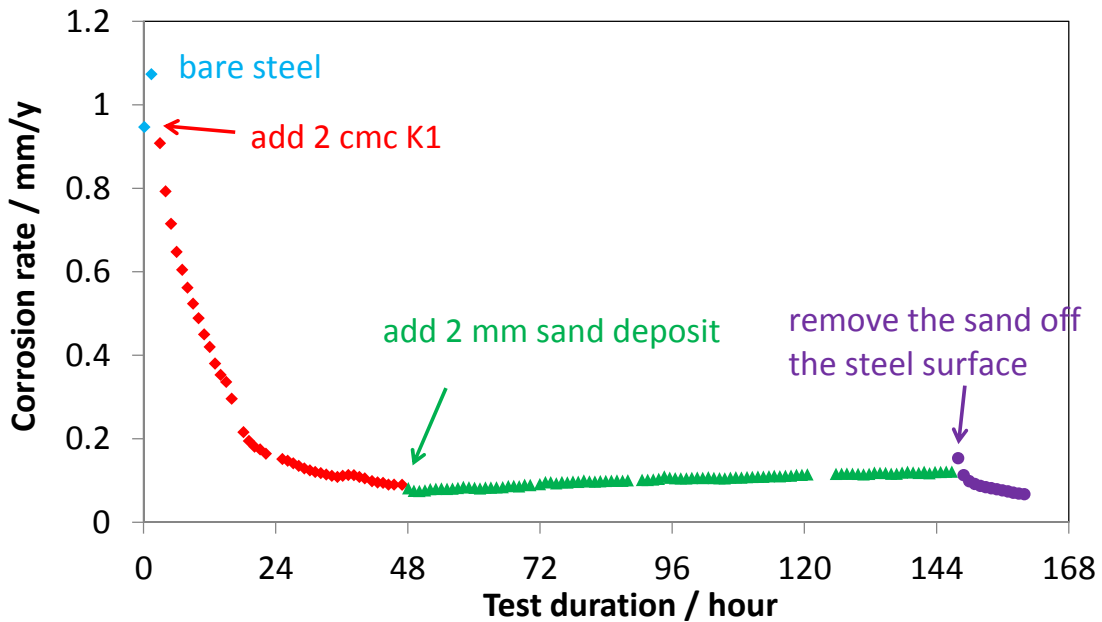


Figure 20 Variation of general corrosion rate with time measured by LPR at test conditions: 1 wt% NaCl solution, bulk pH 5.0, 25°C.

Based on all experimental observations, a localized corrosion mechanism based on a failure to inhibit underneath each individual sand particle can now be proposed. It appears that in the crevices formed between the sand particles and the steel, the inhibitor molecules fail to adsorb and protect the steel surface, while other more open access areas are inhibited. This lack of inhibition is compounded by

formation of galvanic cells which lead to even higher localized corrosion rates underneath each sand particle. Indeed the large numbers of small pits developing underneath each sand particle eventually merge into one large rapidly corroding area underneath the whole sand deposit.

This mechanism can help explain why no change in corrosion rate was measured by LPR when the inhibitor was added. One needs to recall that the corrosion rate calculated from LPR measurement is an average corrosion rate across the whole steel specimen surface. The calculation is based on the assumption that the steel surface corrosion is uniform. However, when a sand deposit is present, the steel surface is not uniformly corroded, because of the high pit penetration rate underneath each sand particle. This localized high corrosion rate is roughly balanced with the low (inhibited) corrosion rate of the adjacent more exposed area, which resulted in the observation of little change in measured LPR general corrosion rate. This also leads to the conclusion that LPR is not a suitable method to monitor corrosion in an under-deposit corrosion study.

Table 4: Summary of cases where pits were found.

Case		Pit penetration rate (IFM)	General corrosion rate (LPR)	Note
Partially covered surface	70%	2.0 mm/y	0.3 mm/y	Inhibitor K1 added after sand
Fully covered surface	1 layer (~ 0.75 mm)	2.0 mm/y	0.2 mm/y	
	2 mm	2.5 mm/y	0.08 mm/y	Inhibitor K1 added before sand

CONCLUSIONS

Based on the results discussed in this work, the following conclusions can be made:

1. A simple and reliable method for testing of localized under-deposit corrosion was developed and verified.
2. Mechanisms for localized corrosion in the presence of solids were identified and explained.
 - a) General depletion of surfactant inhibitor (imidazoline based) by adsorption on silica sand surface is not the critical factor that causes inhibition failure in under-deposit CO₂ corrosion.
 - b) Slow diffusion of inhibitor through the porous sand deposit layer is also not the limiting factor in cases where inhibition failed.
 - c) Pits were found in under-deposit corrosion and related to the inability of the inhibitor to protect the steel surface in the crevices immediately underneath each individual sand particle. These pits propagated very fast due to galvanic effects, eventually merging and causing a high rate of "general" attack underneath sand deposits.

ACKNOWLEDGEMENTS

The authors would like to thank the following companies for financial support: BP, Champion Technologies, Chevron, Clariant Oil Services, ConocoPhillips, ENI S.P.A., ExxonMobil, Inpex

Corporation, NALCO Energy Services, Occidental Petroleum Co., Petrobras, PETRONAS, PTT, Saudi Aramco, Total, TransCanada, MI-SWACO, HESS and WGIM.

REFERENCES

1. J. Huang, B. Brown, X. Jiang, B. Kinsella and S. Nestic, "Internal CO₂ corrosion of mild steel pipelines under inert solid deposits", CORROSION/10, paper no. 379 (Houston, TX: NACE, 2010)
2. A. Pedersen, K. Bilkova, E. Culbrandsen and J. Kvarekval, "CO₂ corrosion inhibitor performance in the presence of solids: test method development", CORROSION/08, paper no. 632 (Houston, TX: NACE, 2008)
3. S. Turgoose, G. E. Dicken and J. W. Palmer, "Review of issues associated with inhibition of scale-deposit-covered pipelines", SPE/2006, paper no. 100728 (Aberdeen, Scotland, U.K., SPE, 2006)
4. H. D. Reus, E. L. J. A. Hendriksen, and M. Wilms, "Test methodologies and field verification of corrosion inhibitors to address under deposit corrosion in oil and gas production systems", CORROSION/05, paper no. 288 (Houston, TX: NACE, 2005).
5. D. I. Horsup, J. C. Clark, B. P. Binks, P. D. I. Fletcher, J. T. Hicks, "I put it in, but where does it go?- the fate of corrosion inhibitors in multiphase systems", CORROSION/07, paper no. 617 (Houston, TX: NACE, 2007).
6. T. D. Place, M. R. Holm, C. Cathrea, T. Ignacz, "Understanding and mitigating large pipe underdeposit corrosion", *Material Performance*, 54, 2009 January
7. A. Turnbull, G. Hinds, P. Cooling, S. Zhou, "A multi-electrode approach to evaluating inhibition of underdeposit corrosion in CO₂ environments", CORROSION/09, paper no. 445 (Houston, TX: NACE 2009)
8. A. Crossland, R/ Woollam, J. Palmer, G. John, S. Turgoose and J. Vera, "Corrosion inhibitor efficiency limits and key factors", CORROSION/11, paper no. 062 (Houston, TX: NACE, 2011)
9. W. H. Durnie, M. A. Gough, J. A. M. de Reus, "Development of corrosion inhibitors to address under deposit corrosion in oil and gas production systems", CORROSION/05, paper no. 290 (Houston, TX: NACE International 2005)
10. C. Canto, "Effect of wall shear stress on inhibitor film" CCJIP Advisory Board Meeting report, October 2009
11. D. A. Jones, Principles and prevention of corrosion, 2nd ed., Prentice Hall, NJ, 1996
12. D.D.N. Singh, and A. Kumar, "A fresh look at ASTM G 1-90 solution recommended for cleaning of corrosion products formed on iron and steels", *Corrosion*, Vol.59, No. 11, 2003
13. V. Jovancicevic, S. Ramachandran, and P. Prince, "Inhibition of Carbon Dioxide Corrosion of Mild Steel by Imidazolines and Their Precursors", *Corrosion*, Vol. 55, No. 05, 1999
14. P. Ho, K. Lehovc and L. Fedotowsky, "Charge motion on silicon oxide surfaces", *Surface Science* 6, 1967
15. W. J. Herzberg and W. R. Erwin, "Gas-chromatographic study of the reaction of glass surfaces with dichlorodimethylsilane and chlorotrimethylsilane", *Journal of Colloid and Interface Sciences*, Vo. 83, No. 1, 1970
16. S. Nestic, J. Postlethwaite, S. Olsen, "An Electrochemical Model for Prediction of Corrosion of Mild Steel in Aqueous Carbon Dioxide Solutions", *Corrosion Science*, Vol. 52, No. 4, 1996